Electronic Supplementary Material (ESI) for Nanoscale.

Supporting Information

Edge-on **and** ***face-on*** **functionalized Pc on enriched semiconducting SWCNT hybrids**

Luis M. Arellano,[a] Luis Martín-Gomis,[b] Habtom B. Gobeze,[c] Desiré Molina[b], Cristina Hermosa,[a] María J. Gómez-Escalonilla,[a] José Luis G. Fierro,[d] Ángela Sastre-Santos,[b,*] Francis D'Souza[c,*] and Fernando Langa[a,*]

[a] *Universidad de Castilla-La Mancha, Instituto de Nanociencia, Nanotecnología y Materiales Moleculares (INAMOL), 45071-Toledo, Spain.*

E-mail: Fernando.Langa@uclm.es

[b] *Área de Química Orgánica, Instituto de Bioingeniería, Universidad Miguel Hernández, Avda. de la Universidad, s/n, Elche 03202, Spain.*

E-mail: asastre@umh.es

[c] *Chemistry and Materials Science and Engineering, University of North Texas, 76203-5017 Denton, TX, USA.*

E-mail: Francis.DSouza@UNT.edu

[d] *Instituto de Catálisis y Petroleoquímica, CSIC, Cantoblanco, 28049, Madrid, Spain.*

E-mail: jlgfierro@icp.csic.es

CONTENTS

Instruments

The thermogravimetric analysis was performed using a TGA/DSC Linea Excellent instrument by Mettler-Toledo, collected under inert atmosphere of nitrogen, with a rate of 10 ºC min^{-1} with a ramp between 40º and 1000 ºC, and the weight changes were recorded as function of temperature. FTIR spectra were carried out using pellets in dried KBr. The instrument used was a Fourier Transform IR spectrophotometer (Avatar 370) in a spectral range from 400 cm^{-1} to 4000 cm^{-1}.

Raman spectroscopy analyses were performed on an inVia Raman microscope (Renishaw) at room temperature, equipped with laser at 785 nm, on solid samples deposited onto a glass coverslip. The laser spot was focused on the sample surface using a long working distance 50X objective. Reported spectra are average of at least five measurements performed in different areas of the sample and normalized to the G-Band. The intensity ratio ID/IG was obtained by taking peak intensities without baseline corrections. The data were analyzed using Origin software.

AFM images were recorded in tapping mode using a Multimode 8 system (Veeco Instruments Inc., Santa Barbara, USA) with a NanoScope V controller (Digital Instruments, Santa Barbara, USA) operating at room temperature in ambient air conditions. RTESP-300 Bruker silicon cantilevers with a resonance frequency of 300 kHz and a nominal force constant of 40 Nm^{-1} were used for AFM measurements. The images were processed using WSxM[1] (freely downloadable scanning probe microscopy software from http://www.wsxmsolutions.com).

Sample preparation:Preparation of Aqueous Dispersed SWCNT: pristine SWCNT and functionalized samples (0.5 mg/mL) were dispersed by ultrasonication (37 kHz, 380 W) in Milli-Q aqueous solution containing 2 wt% sodium dodecylbenzene sulphonate (SDBS) during 120 minutes. To remove the aggregates, the resulting suspensions were centrifuged at 13000 rpm until they had no solid.

Deposition of samples on surface: The samples investigated by AFM were prepared by drop-cast (15 μL) the diluted surfactant solutions onto SiO_2 wafers and left the drop for 20 minutes. This is followed by surfactant removal by washing the substrates generously with Milli-Q water and dried under an argon flow. Prior to deposition, the surfaces were functionalize with (3-aminopropyl) triethoxysilane Milli-Q aqueous solution (0.5% v/v), subsequently washed with 2-propanol and Milli-Q water, and then dried with a stream of argon.

---

[1] I . Horcas, R. Fernandez, J.M. Gómez-Rodriguez, J. Colchero, J. Gómez-Herrero and A. M. Baro, *Rev. Sci. Instrum.* 78, 013705 (2007).

X-ray photoelectron spectra (XPS) were recorded using an Escalab 200R (VG, UK) electron spectrometer equipped with a hemispherical analyzer, operating in the constant pass energy mode, and an MgKα (hν = 1253.6 eV, 1 eV = 1.603 x 10^{-19} J) X-ray source operated at 10 mA and 12 kV. The detection angle of photoelectrons was 60º to the surface of the specimen. The spectrometer was calibrated against Au4$f_{7/2}$ line at 84.0 eV using a gold sheet and Cu2$p_{3/2}$ at 932.5 eV from a copper sheet. Charge effects on the samples were removed by taking the C1s line from adventitious carbon at 284.8 eV. In order to estimate the photoelectron peak intensities, the background was subtracted from the measured spectra according to the Shirley method and using a combination of Gaussian and Lorentzian lines (90G-10L). The relative surface atomic ratios were determined from the corresponding peak intensities, corrected with tabulated atomic sensitivity factors. The reproducibility of the results was confirmed several times under the same conditions.

Osteryoung Square Wave Voltammetry (OSWV) was performed in benzonitrile solution. Tetrabutylammonium hexafluorophosphate ($TBAPF_6$) (0.1 M), used as supporting electrolyte, was purchased from Aldrich-Sigma and used without purification. Solutions were deoxygenated by argon bubbling prior to each experiment, which was run under argon atmosphere. Experiments were done in a one-compartment cell equipped with a carbon working electrode (diameter = 2 mm) and a platinum wire counter electrode. A scan rate of 0.1 V.s^{-1} was used. An $Ag/AgNO_3$ electrode was used as reference and checked against the ferrocene/ferrocenium couple (Fc/Fc^+) before and after each experiment.

UV-vis spectra were measured on a Shimatzu UV 3600 spectrophotometer.

Steady-state emission spectra (1D and 3D) and fluorescence lifetimes were evaluated by using a Horiba Yvon Nanolog coupled with time-correlated single photon counting with nanoLED excitation sources. A right angle detection method was used.

Femtosecond transient absorption spectroscopy experiments were performed using an Ultrafast Femtosecond Laser Source (Libra) by Coherent incorporating diode-pumped, mode locked Ti:Sapphire laser (Vitesse) and diode-pumped intra cavity doubled Nd:YLF laser (Evolution) to generate a compressed laser output of 1.45 W. For optical detection, a Helios transient absorption spectrometer coupled with femtosecond harmonics generator both provided by Ultrafast Systems LLC was used. The source for the pump and probe pulses were derived from the fundamental output of Libra (Compressed output 1.45 W, pulse width 100 fs) at a repetition rate of 1 kHz. 95% of the fundamental output of the laser was introduced into a TOPAS-Prime-OPA system with 290-2600 nm tuning range from Altos Photonics Inc., (Bozeman, MT), while the rest of the output was used for generation of white light continuum. In the present study, the second harmonic 400 nm excitation pump was used in all the experiments.

Kinetic traces at appropriate wavelengths were assembled from the time-resolved spectral data. Data analysis was performed using Surface Xplorer software supplied by Ultrafast Systems. All measurements were conducted in degassed solutions at 298 K.

TGA results

The comparison of the thermogravimetric profiles of *pristine* and *functionalized* SWCNTs HiPco gave a first evidence of the sidewall functionalization of carbon nanotubes (Figure S1). The thermogram presented in Figure S1 arevealed a weight loss about 11.1 % for SWCNT HiPco, 29.8 % for TMS derivative, 42.5 % for *functionalized* ZnPc-SWCNT and 52.7 % for ZnPc, under at inert atmosphere and in the 40-650 ºC temperature range. The corrected weight losses due to the functional groups on nanotubes were the estimated to be 18.7 % for SWCNT-TMS and about 31.4 % for Zn-Pc-SWCNT HiPco (weight losses difference of SWCNT-TMS - SWCNT HiPco and Zn-Pc-SWCNT HiPco – SWCNT HiPco). Accordingly, the number of trimethyl(phenylethynyl)silane functional groups in SWCNT-TMS was estimated as 1 per 70 carbon atoms; based on these values, we estimated the amount of functional groups in ZnPc- SWCNT HiPco hybrid as 1 per 199 carbon atoms. In the case of Si-Pc- SWCNT HiPco, (see Figure S1b) the thermogravimetric analysis revealed a corrected weight loss of 18.7 % and 33.4 % for SWCNT-TMS and Si-Pc-SWCNT HiPco, respectively. This value corresponds to the presence of one functional group for about 70 C atoms in SWCNT-TMS and 248 C atoms in *functionalized* Si-Pc-SWCNT HiPco.

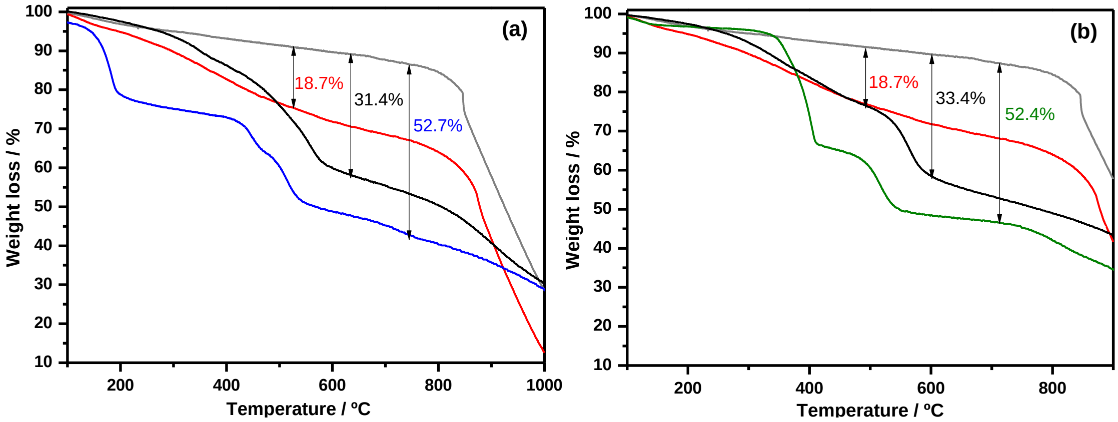

Figure S1. TGA profiles of (a) SWCNT-TMS (—), Zn-Pc-SWCNT Hipco (—) and ZnPc (—) and (b) SWCNT-TMS (—), Si-Pc-SWCNT Hipco (—) and SiPc (—). The TGA data for starting material SWCNT HiPco (—) is also provided for reference in each plot. Heating rate: 10 ºC min^{-1}, atmosphere: Ar.

The termogravimetric analyses (TGA) were also performed on Pcs-(n,m) SWCNTs hybrids (see Figure S2). The TGA graphs for Pcs and *functionalized* SWCNT (n,m) materials, namely (6,5) and (7,6), are compared in Figure S2. For SWCNT (6,5), nearly 39.4% of the weight loss was observed at 650 ºC for ZnPc and 23.7% for SiPc, corresponding to the organic fragments. Using this information, we estimated the amount of functional groups in Zn-Pc-SWCNT (6,5) hybrid as one per 160 C atoms whereas one Pc moiety per 351 carbon atoms in the case of Si-Pc-SWCNT (6,5) hybrid (Figures S2a and 2b). In the case of SWCNT (7,6) hybrids, an average loss value at around 31.8% was found in the case of ZnPc (at 650 ºC) (see Figure S2c). This means that one organic unit is grafted per every 200 carbon atoms in Zn-Pc-SWCNT (7,6).

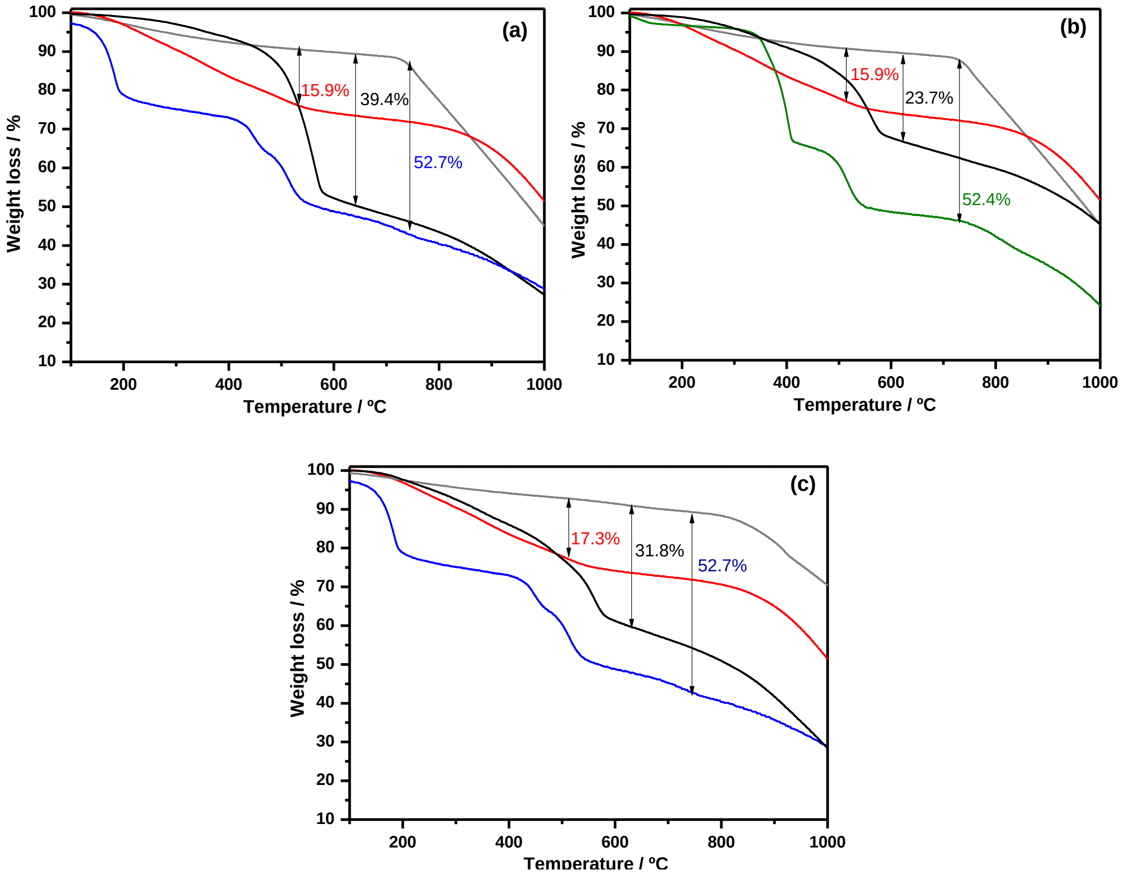

Figure S2. TGA profiles for: (a) SWCNT-TMS (—), Zn-Pc-SWCNT (6,5) (—) and ZnPc (—); (b) SWCNT-TMS (—), Si-Pc-SWCNT (6,5) (—) and SiPc (—) and (c) SWCNT-TMS (—), Zn-Pc-SWCNT (7,6) (—) and ZnPc (—) (40–1000 ºC temperature range). The TGA data for starting materials, SWCNT (6,5) and SWCNT (7,6) (—)is also provided for reference in each plot. Heating rate: 10 ºC min^{-1}, atmosphere: Ar.

XPS studies

The C 1s peak of *pristine* SWCNTs (HiPco and enriched) was satisfactorily fitted to four expected components (see Table S2) at around 284.8, 286.2 and 287.8 eV, which correspond to sp^2 C-C, C-O, and C=O surface functionalities, respectively. In addition, pristine SWCNTs display the π-π* shake up structure, which is indicative of highly ordered carbon nanotube structures. This result suggests that *pristine* SWCNTs possesses some O-containing functional group,[1] which is in agreement with our TGA results as well as previous study[2] (see Figure S3).The quantitative fractions of the oxygen-containing functional groups in the pristine SWCNT is between 2.5 and 4.3 %.

Successful functionalization of the SWCNT surface with TMS is demonstrated by the appearance of Si 2p peak whose binding energy of 101.3 eV is typical of Si-C bonds (see Table S2). As judging from the extent of TMS functionalization (0.6-1.8 % Si atoms), an equivalent amount of C-C triple bonds is expected to be present (see Table S3). This very low proportion of hybridized sp C orbitals did not allow us discriminate a small C 1s component at a binding energy about 284 eV, strongly overlapping on the tail of the intense sp^2 C 1s component of the SWCNT structure (see Figure S4).

Compositional data obtained from the XPS analysis of *functionalized* SWCNTs are reported in Table S3 and Figures S5-S6. As expected, the presence of N atoms and Zn or Si atoms in final *functionalized* SWCNTs materials confirmed the effectiveness of Sonogashira cross coupling as a synthetic route in the introduction of phthalocyanine units on the SWCNT surface. As example, Figure S7 shows the XPS spectra of C1s, N 1s and Zn 2p regions for enriched (6,5) SWCNT *functionalized* with I-ZnPc. In the C 1s region (Figure S7a) is appreciated the sp^3 peak attributed to the phthalocyanine moiety component. Following peak assignment was done based on data reported in bibliography,[3] the high-resolution N1s peak can be curve-fitted in two components: one component at 398.8/399.1 eV associated to pyridyl N and another at 400.3/400.4 eV due to pyrrolic N as observed in Figure S7b, the former peak is three times more intense than the latter. Finally, in agreement with the structure of ZnPc-SWCNT (6,5) hybrid, the Zn 2p peak is also detected at 1021.3 eV peak (Figure S7c). All these results are in full agreement with the TGA results and according with the values shown in Table S3.

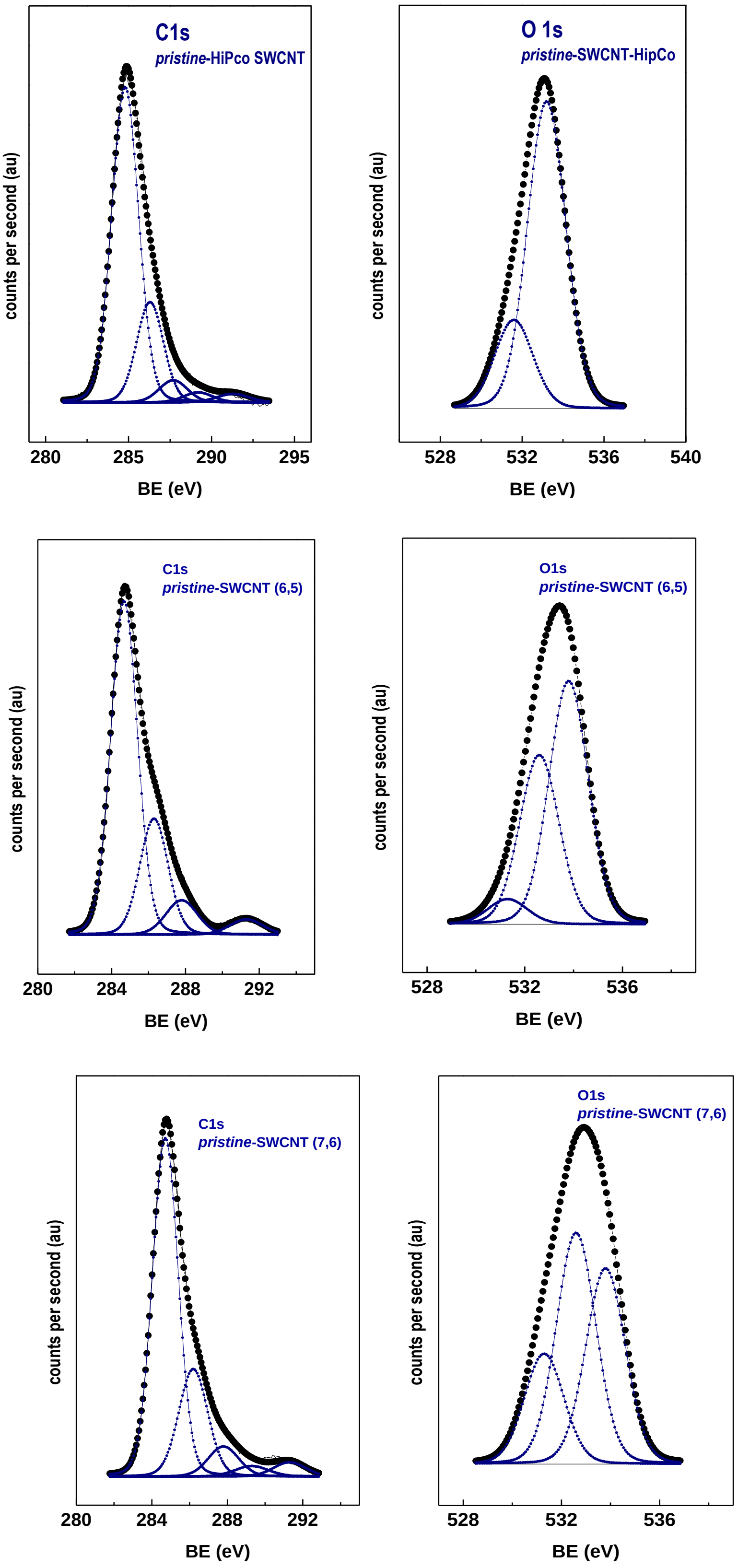

Figure S3. C1s and O1s core-level spectra of starting SWCNTs (HiPco and enriched).

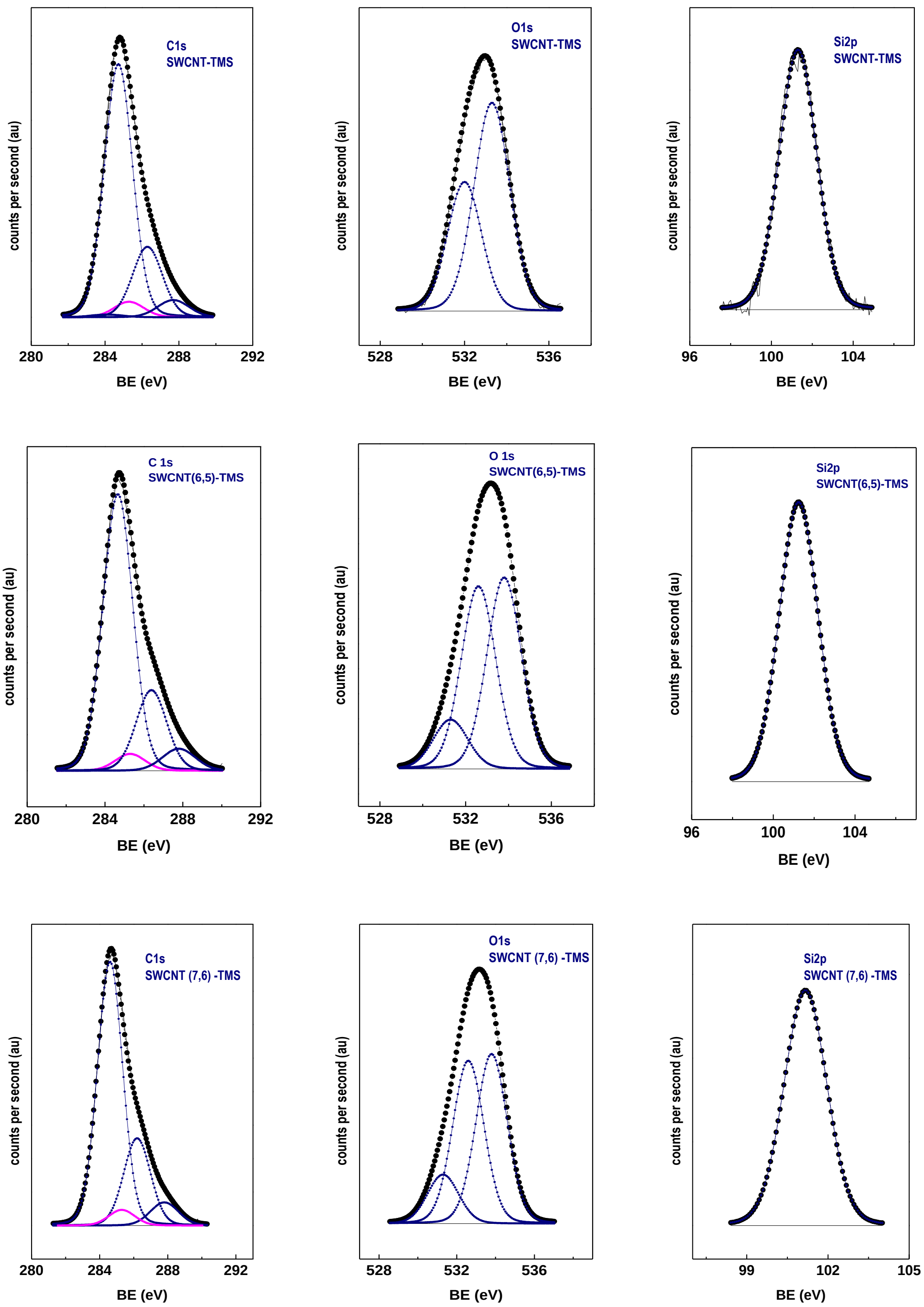

Figure S4. C1s, O1s and Si 2p core-level spectra of SWCNT-TMS (HiPco and enriched) samples.

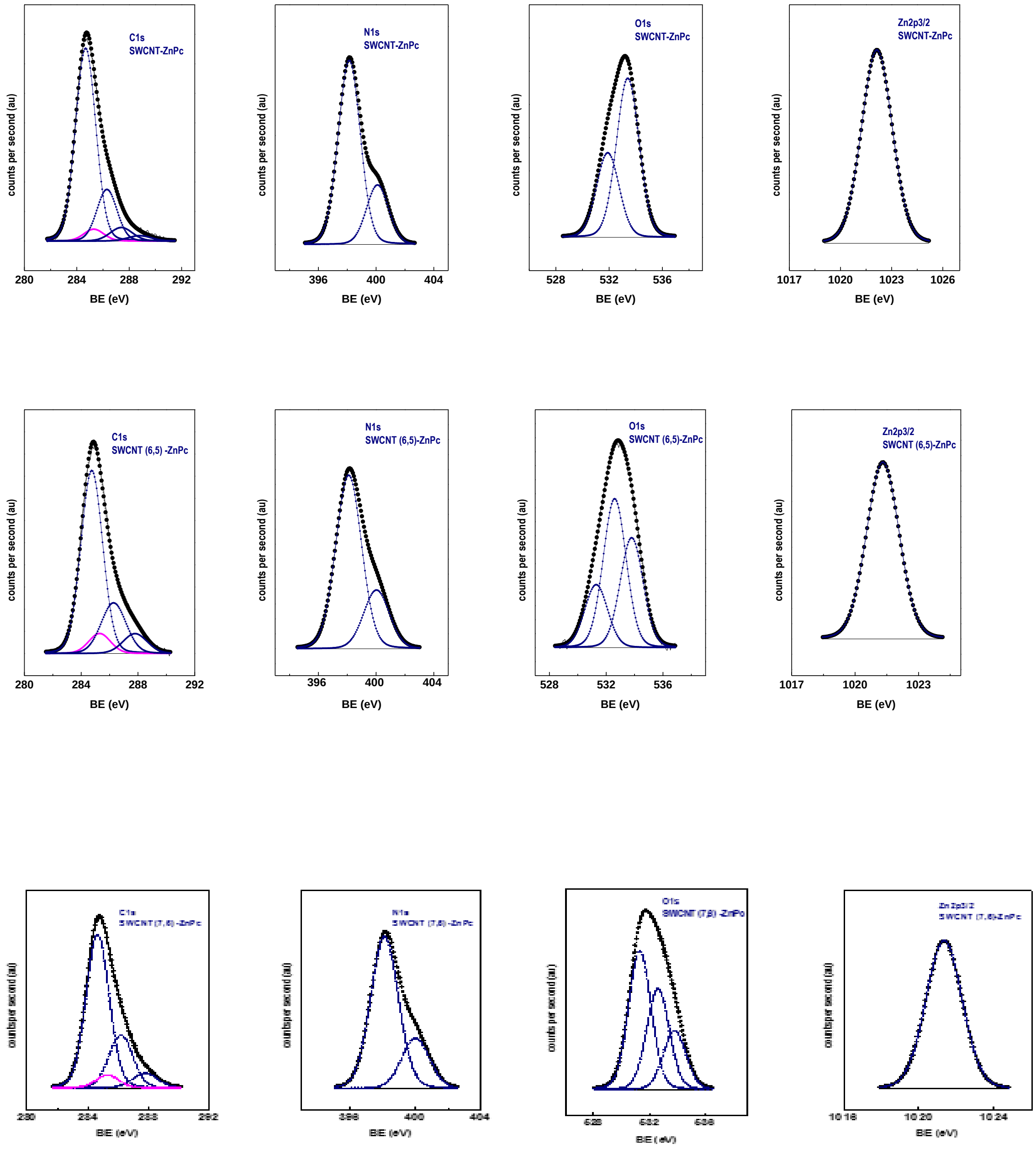

Figure S5. C1s, O1s and Zn 2p core-level spectra of *funtionalized*- HiPCo SWCNT, SWCNT (6,5) and SWCNT (7,6) with ZnPc.

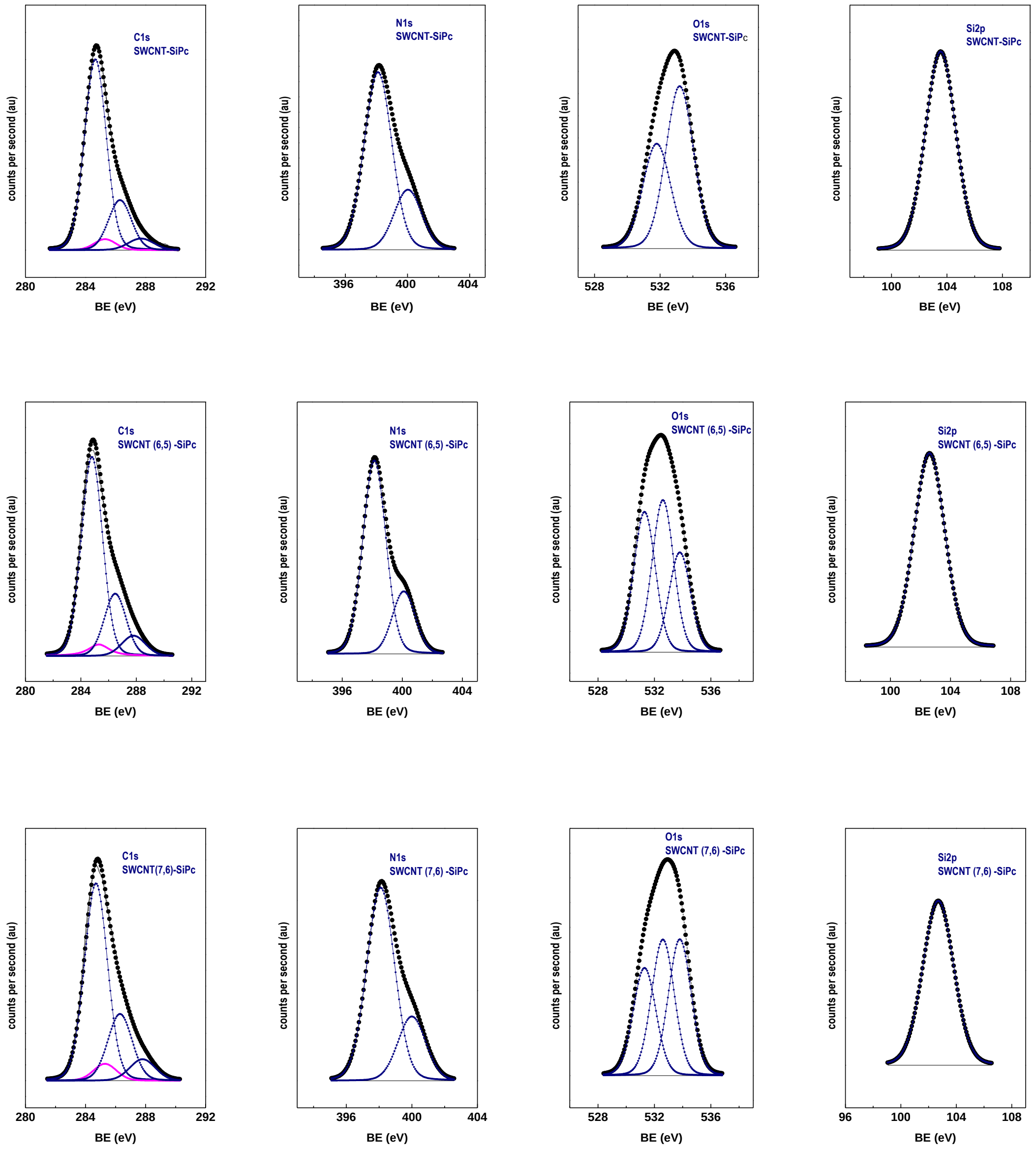

Figure S6. C1s, O1s and Si 2p core-level spectra of *funtionalized* SWCNT HiPco, SWCNT (6,5) and SWCNT (7,6) with SiPc.

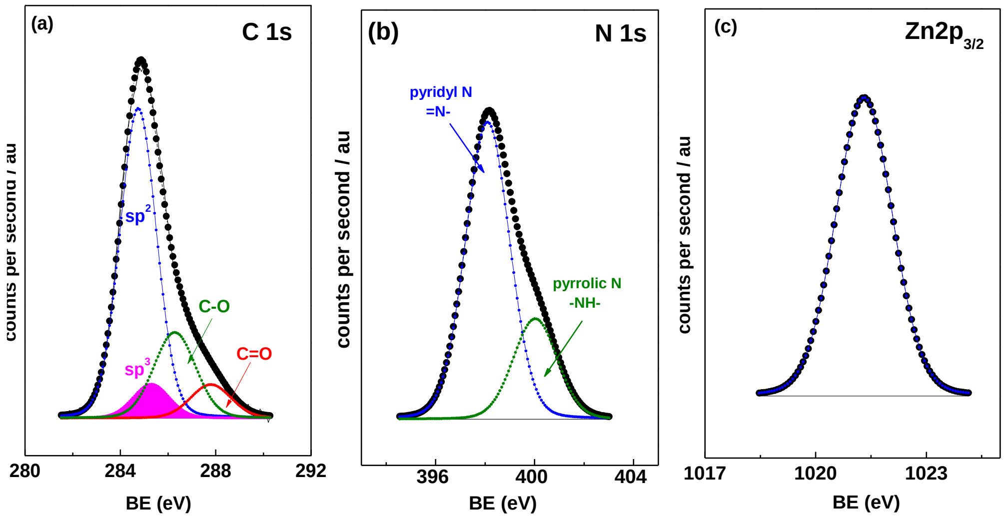

Figure S7. Photoemission spectra and fit of the (a) C1s region (b) N 1s region and (c) Zn 2p region of Zn-Pc-SWCNT (6,5) hybrid material.

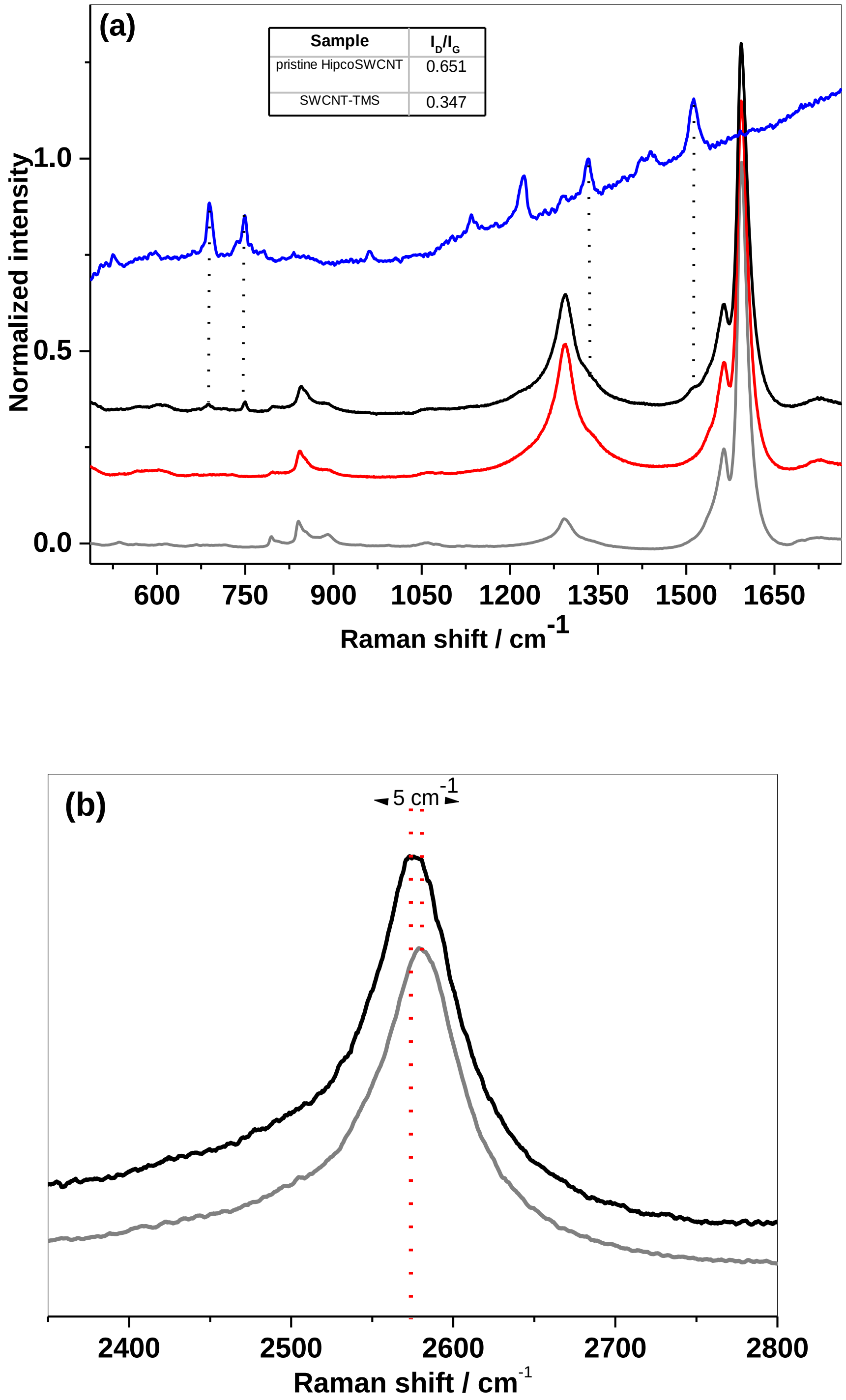

Figure S8. (a) Zoom of Raman spectra of (a) ZnPc-SWCNT HiPco (—), SWCNT-TMS (—), pristine SWCNT HiPco (—) and ZnPc (—). Intensities have been normalized to the G-band (higher frequency); (b) Comparison of 2D-band of pristine SWCNT HiPco (—) and nanohybrid ZnPc-SWCNT HiPco (—). Excitation: 785 nm. Table inserted compares the I_D/I_G ratio between different samples.

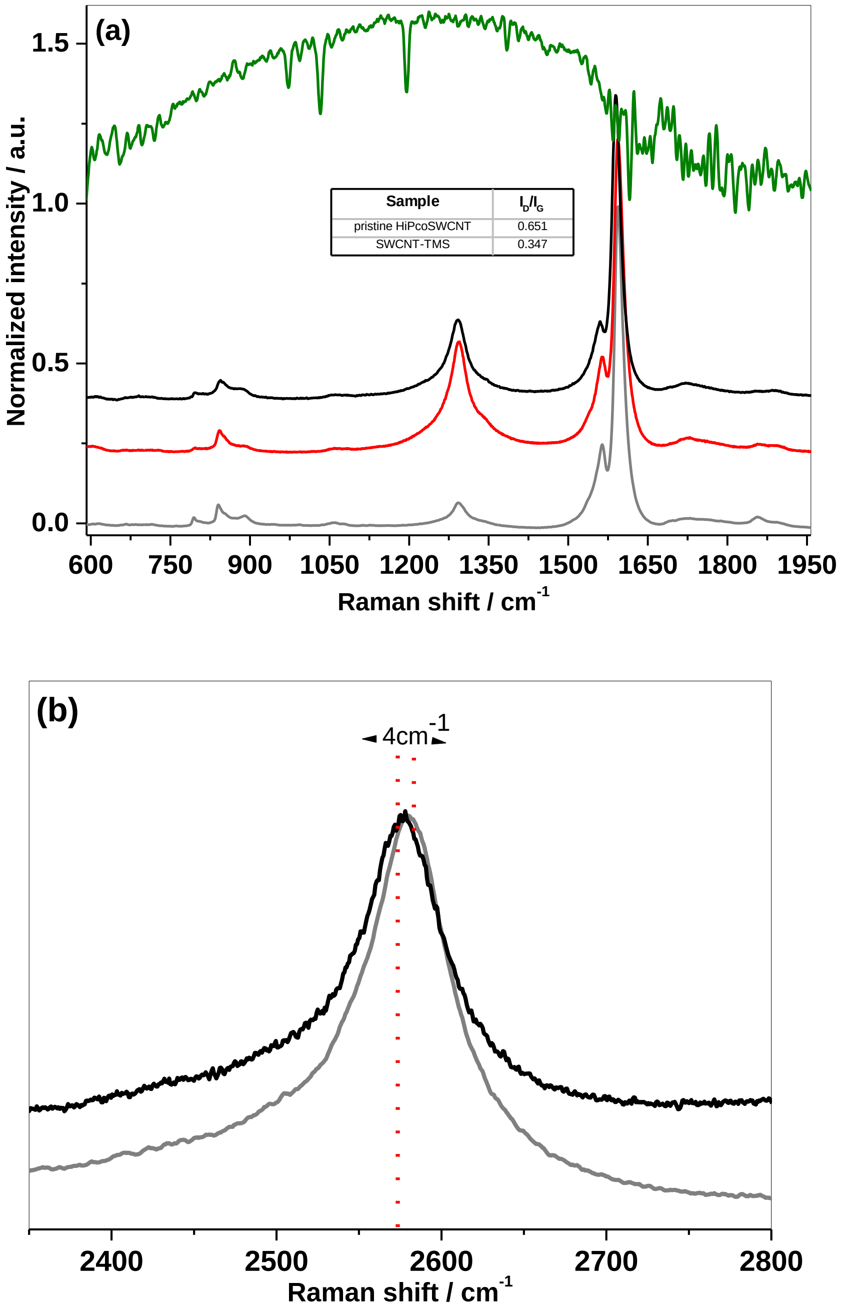

Sample	I_D/I_G
pristine HiPcoSWCNT	0.651
SWCNT-TMS	0.347

Figure S9. (a) Zoom of Raman spectra of (a) SiPc-SWCNT HiPco (—), SWCNT-TMS (—), pristine SWCNT HiPco (—) and SiPc (—). Intensities have been normalized to the G-band (higher frequency); (b) Comparison of 2D-band of pristine SWCNT HiPco (—) and nanohybrid SiPc-SWCNT HiPco (—). Excitation: 785 nm. Table inserted compares the I_D/I_G ratio between different samples.

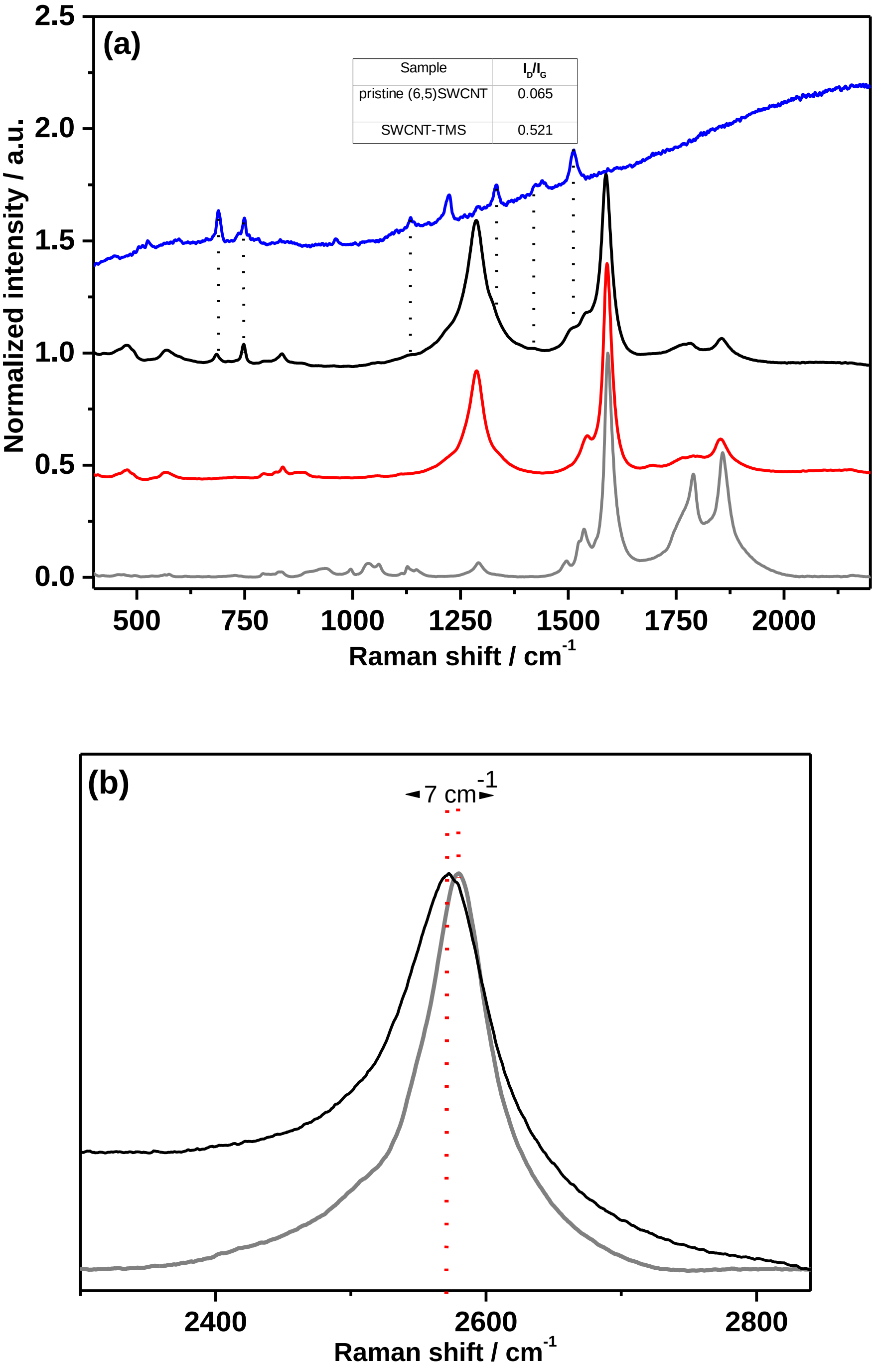

Figure S10. (a) Zoom of Raman spectra of (a) ZnPc-SWCNT (6,5**)** (—), SWCNT-TMS (—), pristine SWCNT (6,5) (—) and ZnPc (—). Intensities have been normalized to the G-band (higher frequency); (b) Comparison of 2D-band of pristine SWCNT (6,5) (—) and nanohybrid ZnPc-SWCNT (6,5) (—). Excitation: 785 nm. Table inserted compares the I_D/I_G ratio between different samples.

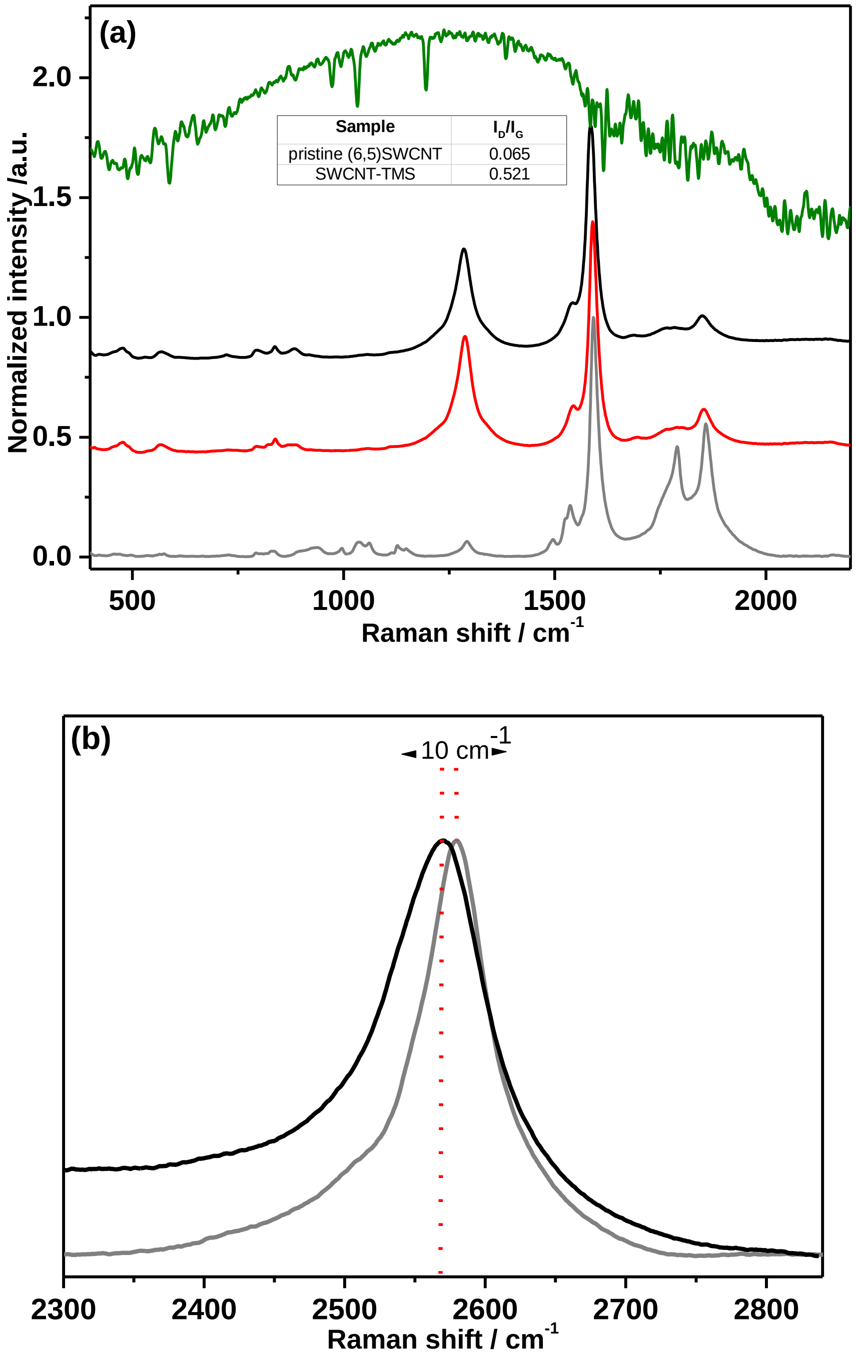

Figure S11. (a) Zoom of Raman spectra of (a) SiPc-SWCNT (6,5) (—), SWCNT-TMS (—), pristine SWCNT (6,5) (—) and SiPc (—). Intensities have been normalized to the G-band (higher frequency); (b) Comparison of 2D-band of pristine SWCNT (6,5) (—) and nanohybrid SiPc-SWCNT (6,5) (—). Excitation: 785 nm. Table inserted compares the I$_D$/I$_G$ ratio between different samples.

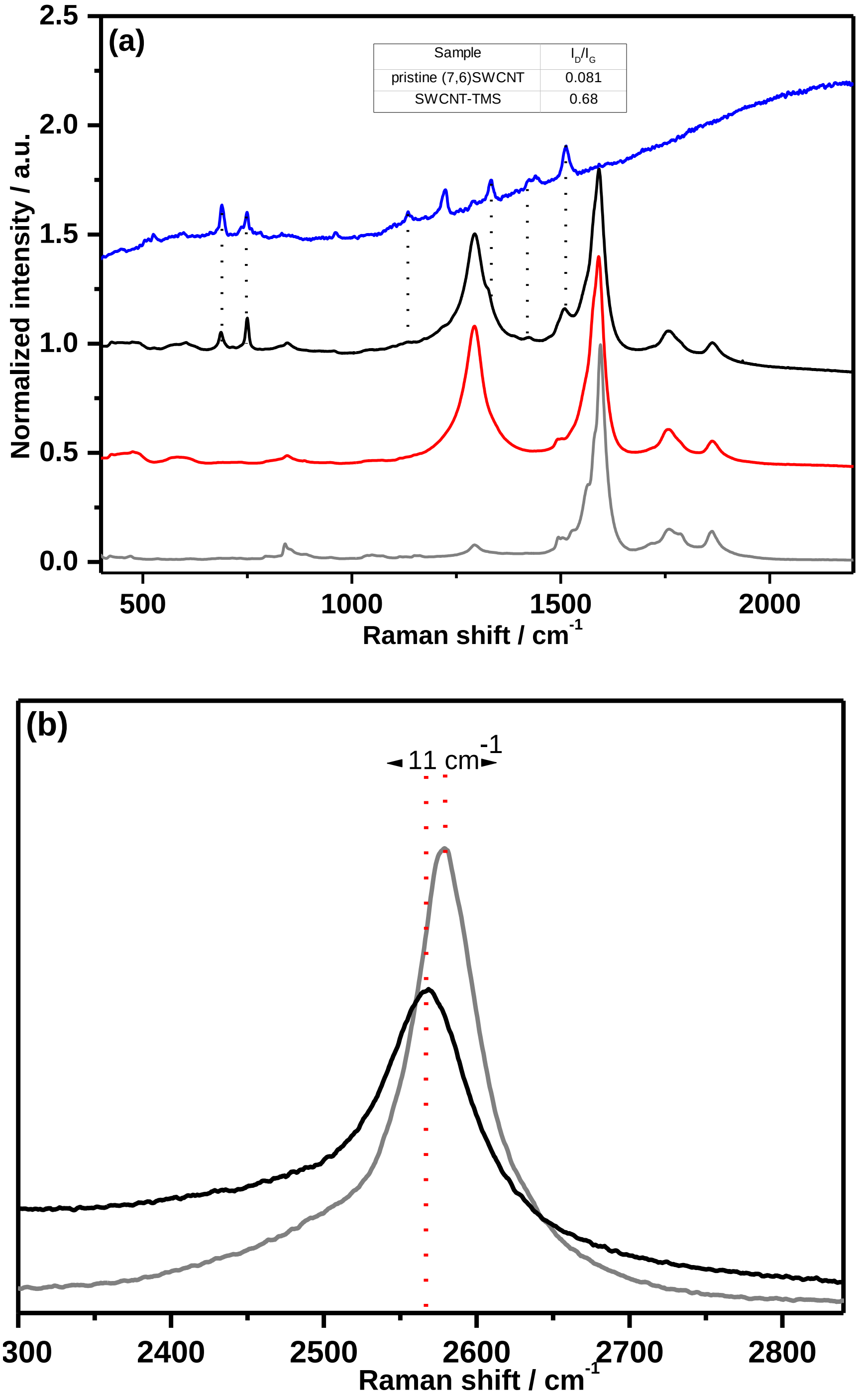

Sample	I_D/I_G
pristine (7,6)SWCNT	0.081
SWCNT-TMS	0.68

Figure S12. (a) Zoom of Raman spectra of (a) ZnPc-SWCNT (7,6) (—), SWCNT-TMS (—), pristine SWCNT (7,6) (—) and ZnPc (—). Intensities have been normalized to the G-band (higher frequency); (b) Comparison of 2D-band of pristine SWCNT (7,6) (—) and nanohybrid ZnPc-SWCNT (7,6) (—). Excitation: 785 nm. Table inserted compares the I_D/I_G ratio between different samples.

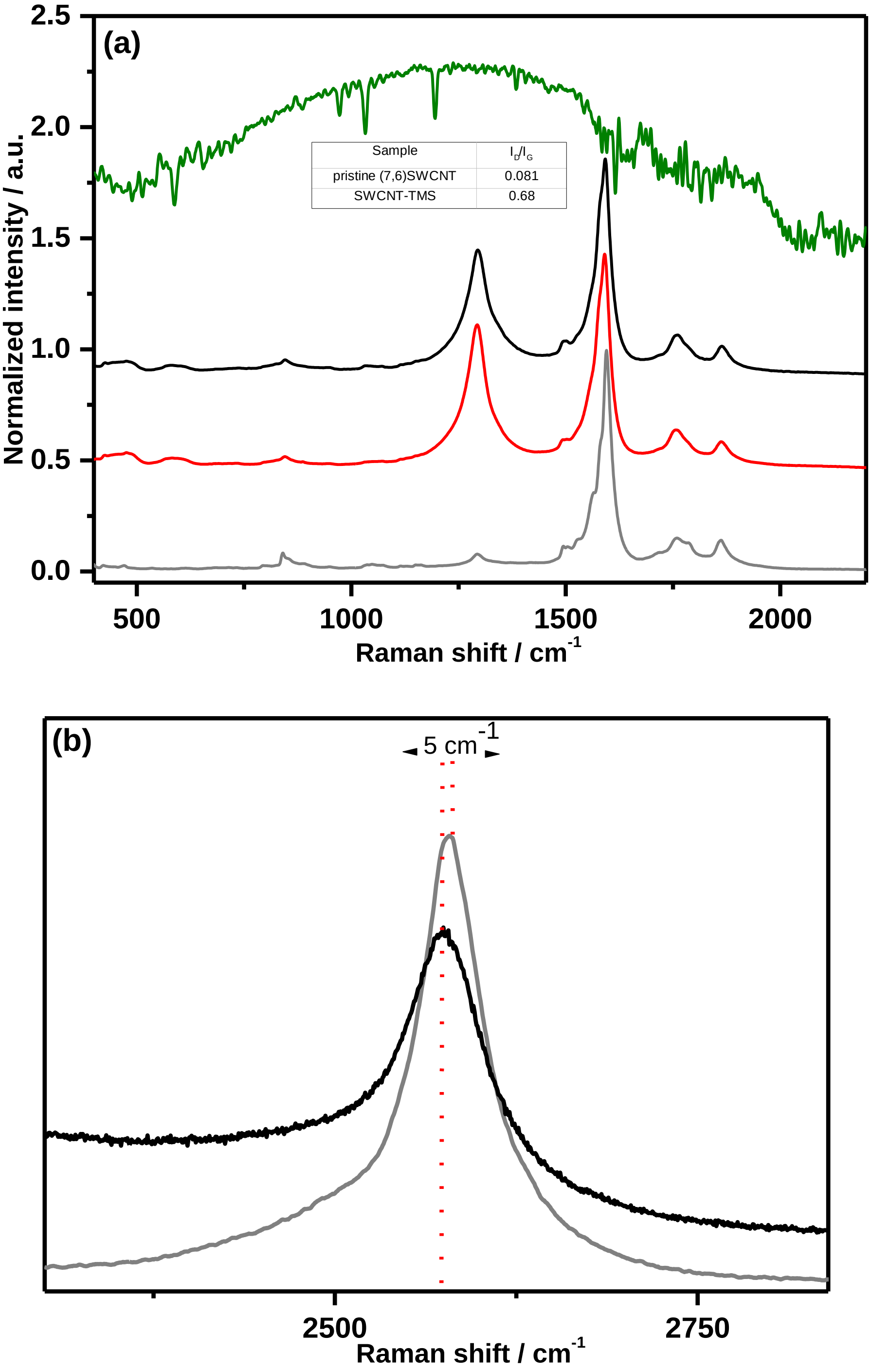

Sample	I_D/I_G
pristine (7,6)SWCNT	0.081
SWCNT-TMS	0.68

Figure S13. (a) Zoom of Raman spectra of (a) SiPc-SWCNT (7,6) (—), SWCNT-TMS (—), pristine SWCNT (7,6) (—) and SiPc (—). Intensities have been normalized to the G-band (higher frequency); (b) Comparison of 2D-band of pristine SWCNT (7,6) (—) and nanohybrid SiPc-SWCNT (7,6) (—). Excitation: 785 nm. Table inserted compares the I_D/I_G ratio between different samples.

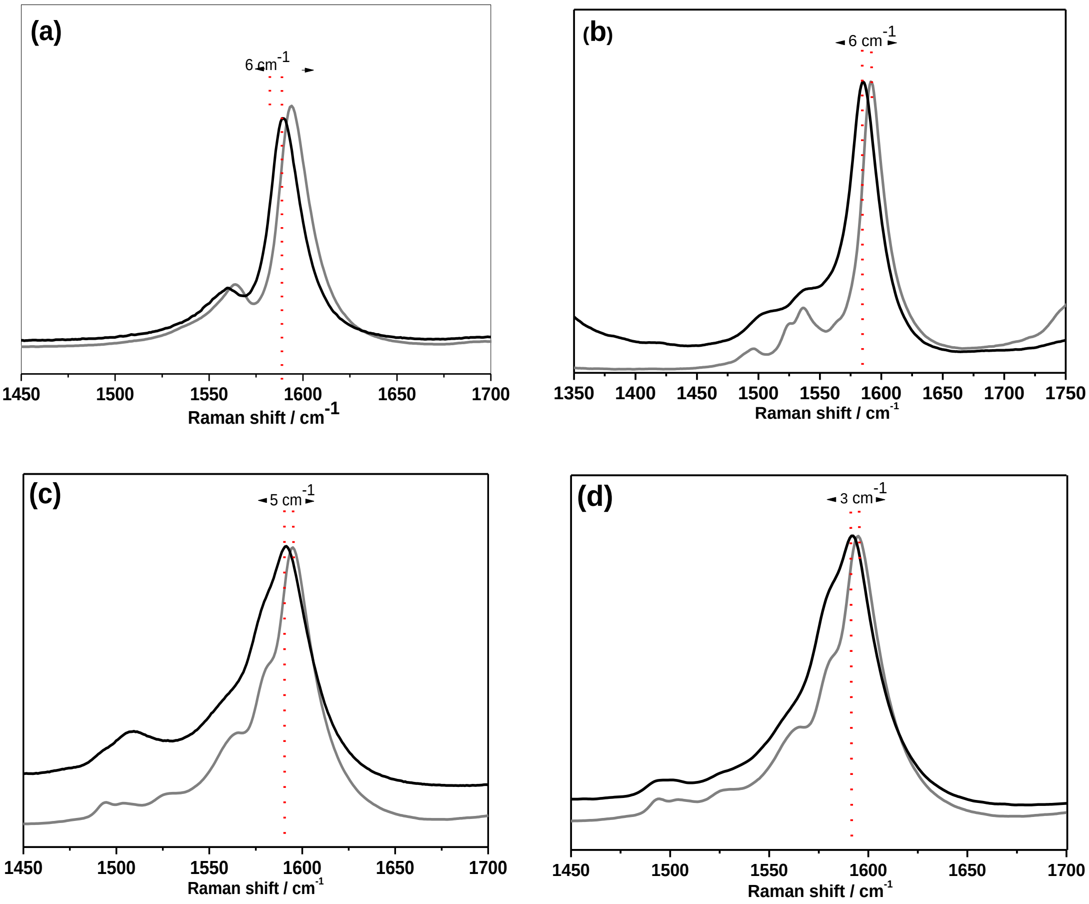

Figure S14. Comparison of the G-band of (a) *pristine* SWCNT HiPco (—) and SiPc-SWCNT HiPco (—); (b) *pristine* SWCNT (6,5) (—) and ZnPc-SWCNT (6,5) (—); (c) *pristine* SWCNT (7,6) (—) and ZnPc-SWCNT **(7,6)** (—) and (d) *pristine* SWCNT (7,6) (—) and SiPc-SWCNT (7,6) (—) (laser excitation = 785 nm).

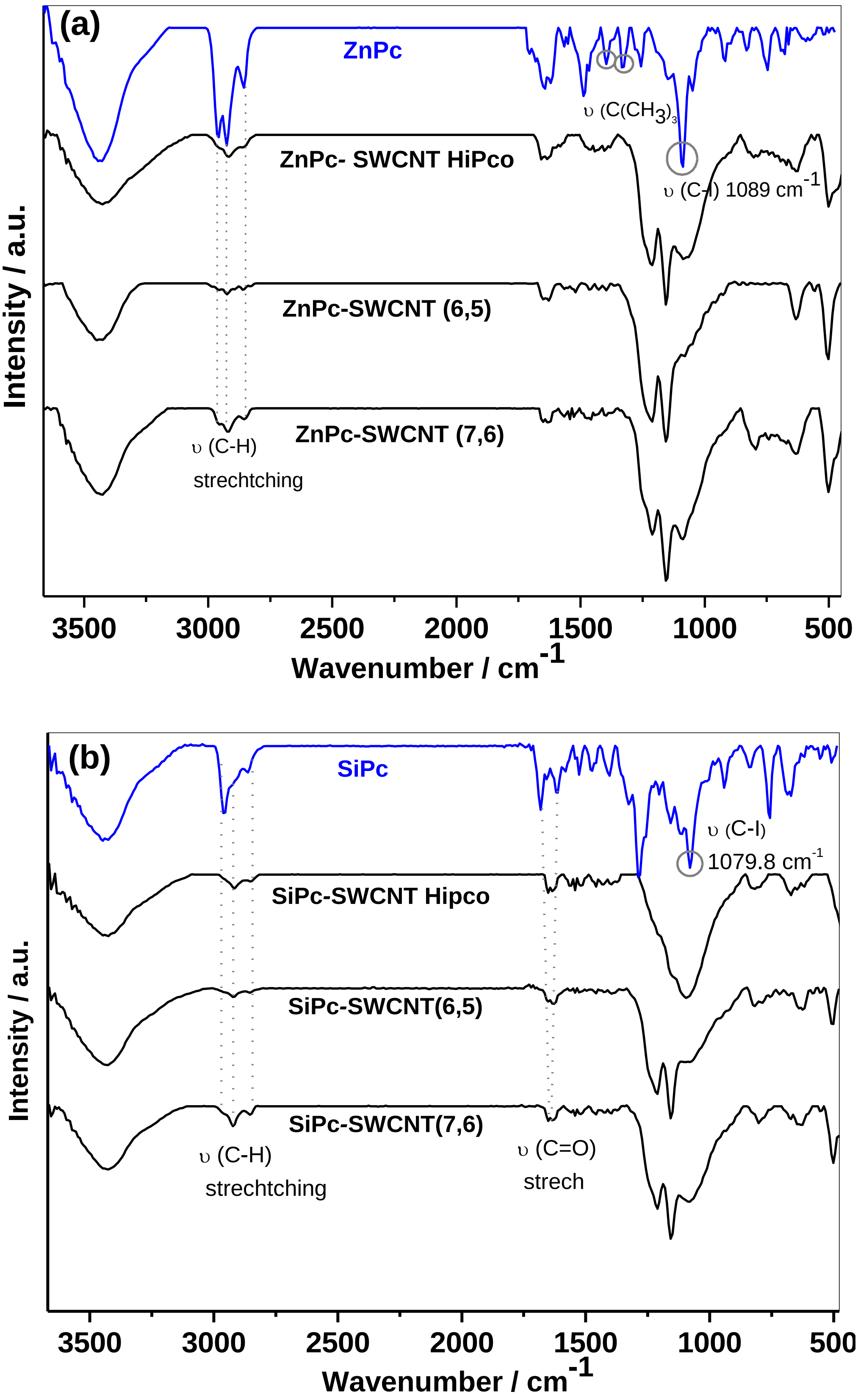

Figure S15. FTIR spectra of *functionalized* HiPco and enriched SWCNTs compared with the corresponding ZnPc (a) and SiPc (b).

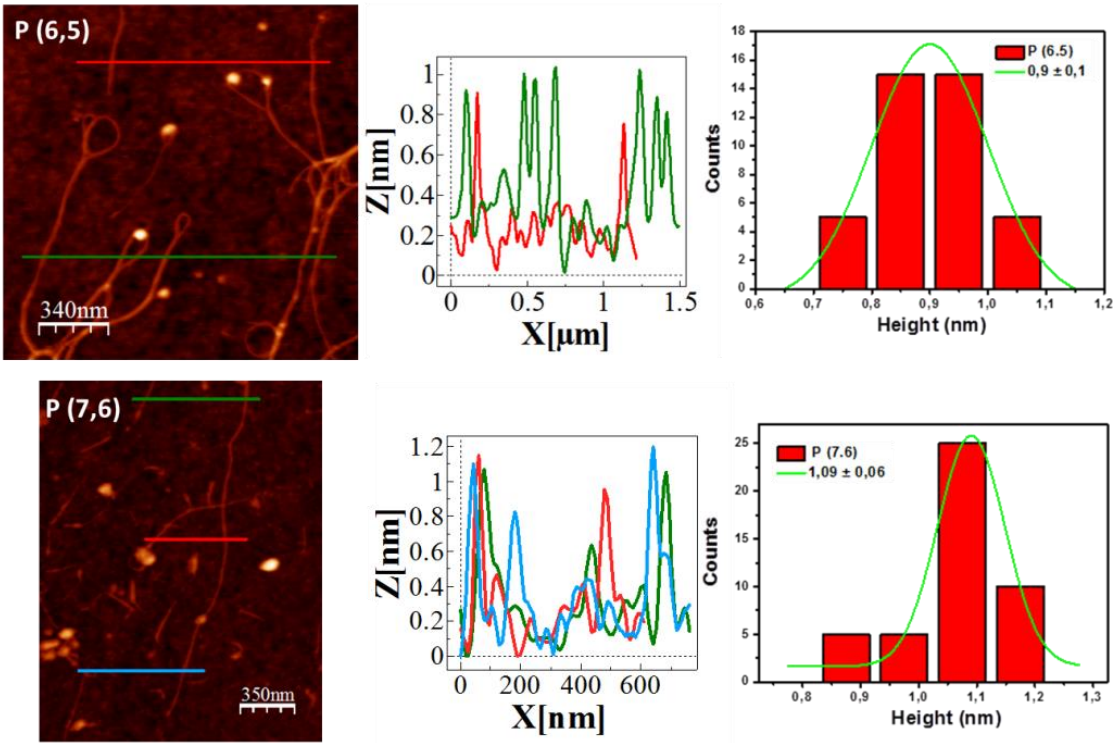

Fig. S16. AFM images and height profiles along the regions indicated for *pristine* SWCNT (6,5) and (7,6) together with their height distribution histogram showing the diameter distribution of the sample.

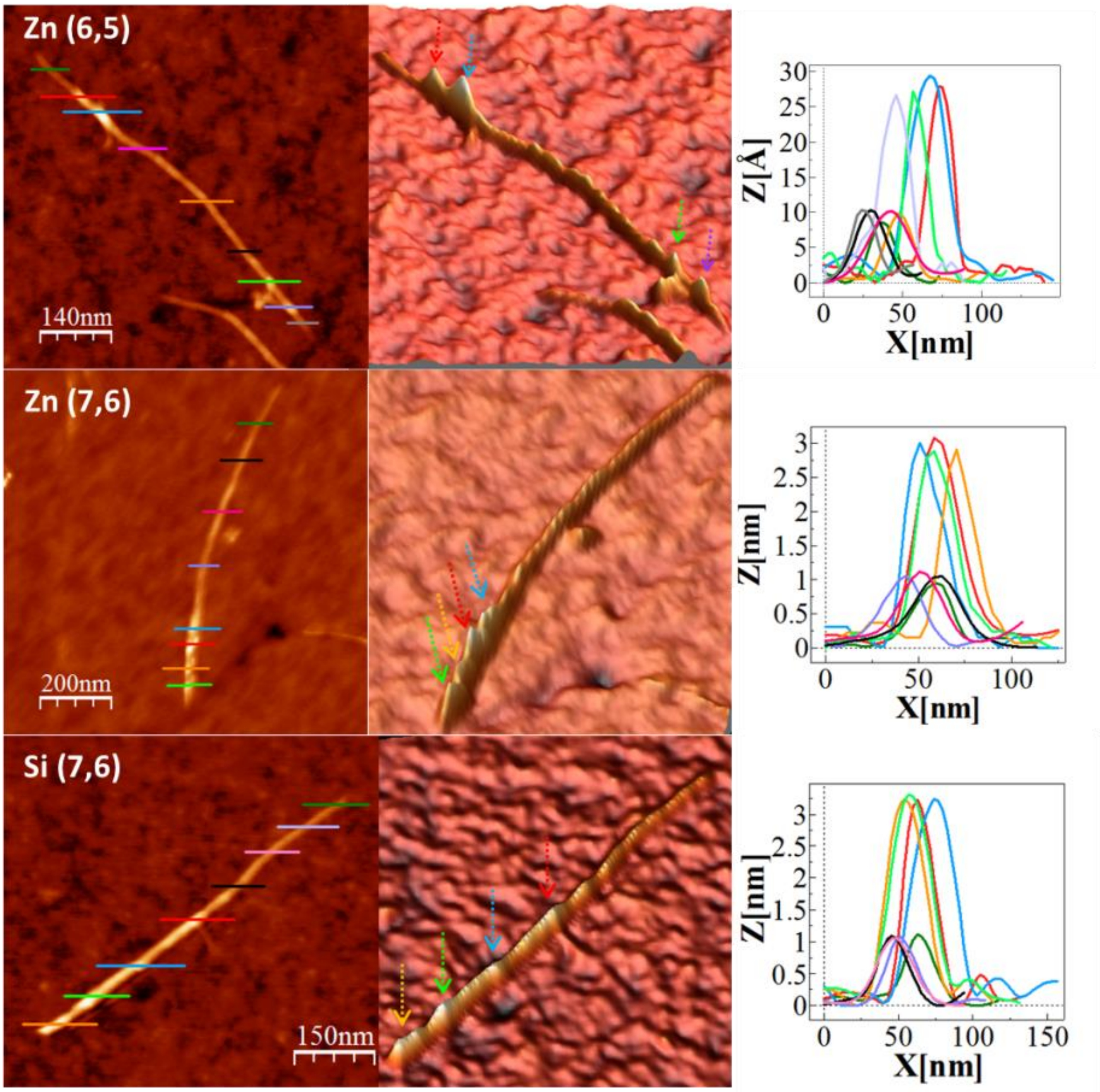

Fig. S17. AFM topographic (left) and 3-dimensional (right) images and height profiles along the regions indicated for Zn (6,5), Zn (7,6) and Si (7,6) hybrids isolated on a SiO_2 surface. The colour code is according with the images.

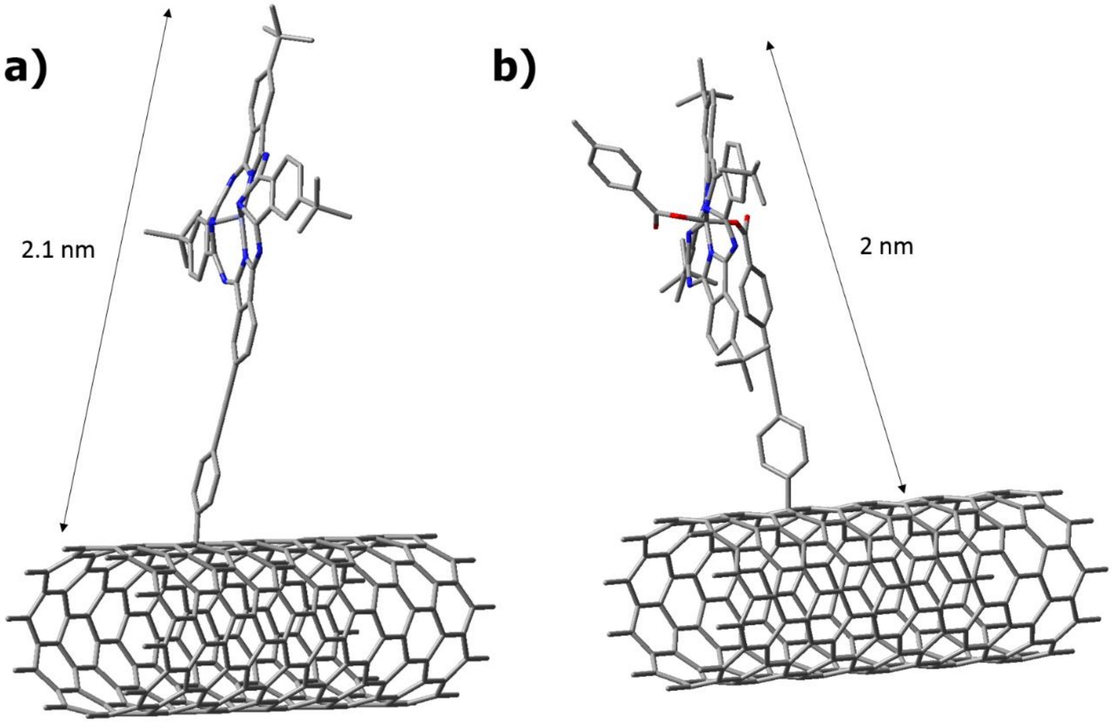

Fig. S18. Modelling structures optimized using semiempirical PM3 method implemented on HyperChem 8.0 program package for (a) ZnPc-SWCNT hybrids and (b) SiPc-SWCNT hybrids.

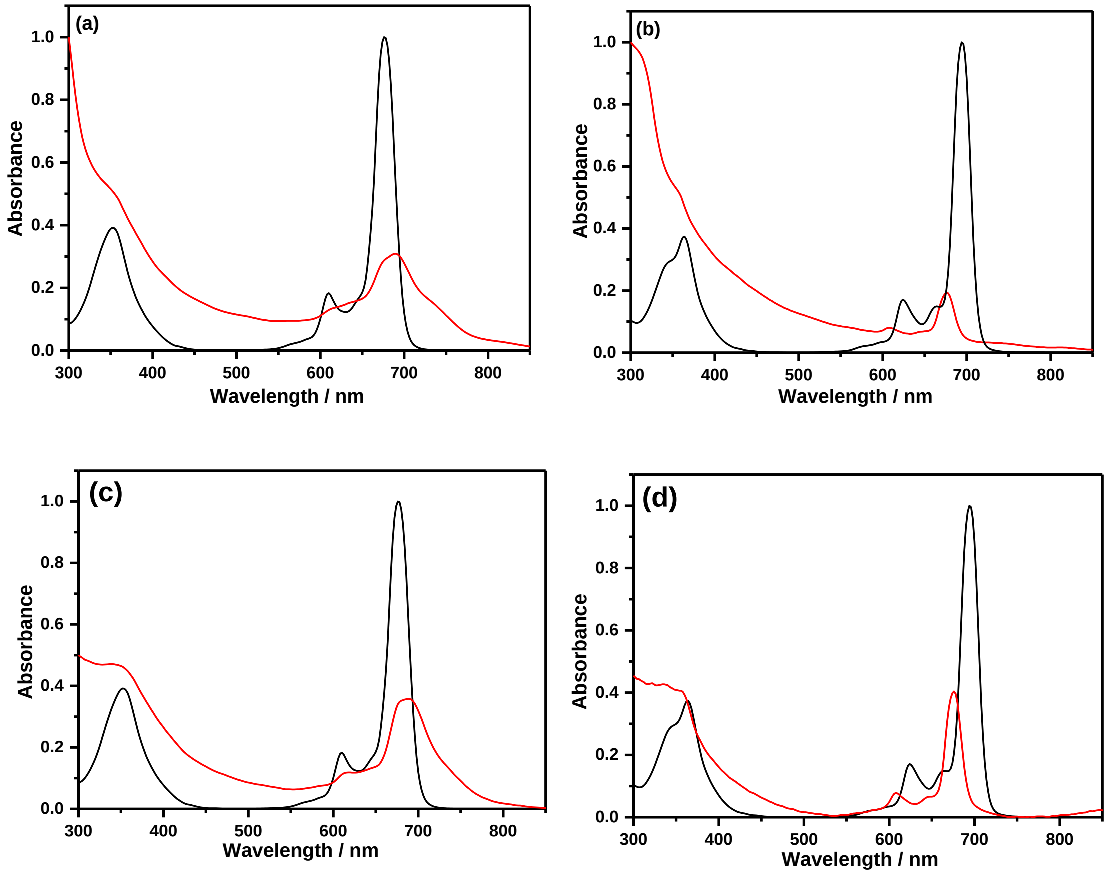

Figure S19. Steady-state absorption spectra of: (a) ZnPc (—) and ZnPc-SWCNT HiPco (—), (b) SiPc (—) and SiPc-SWCNT HiPco (—); (c) ZnPc (—) and ZnPc-SWCNT (6,5) (—) and (d) SiPc (—) and SiPc-SWCNT (6,5) (—), registered in DMF. Measured in isoabsorbing solutions (O.D. = 0.300) (λ_{exc}= 607 nm for ZnPc; λ_{exc}= 624 nm for SiPc).

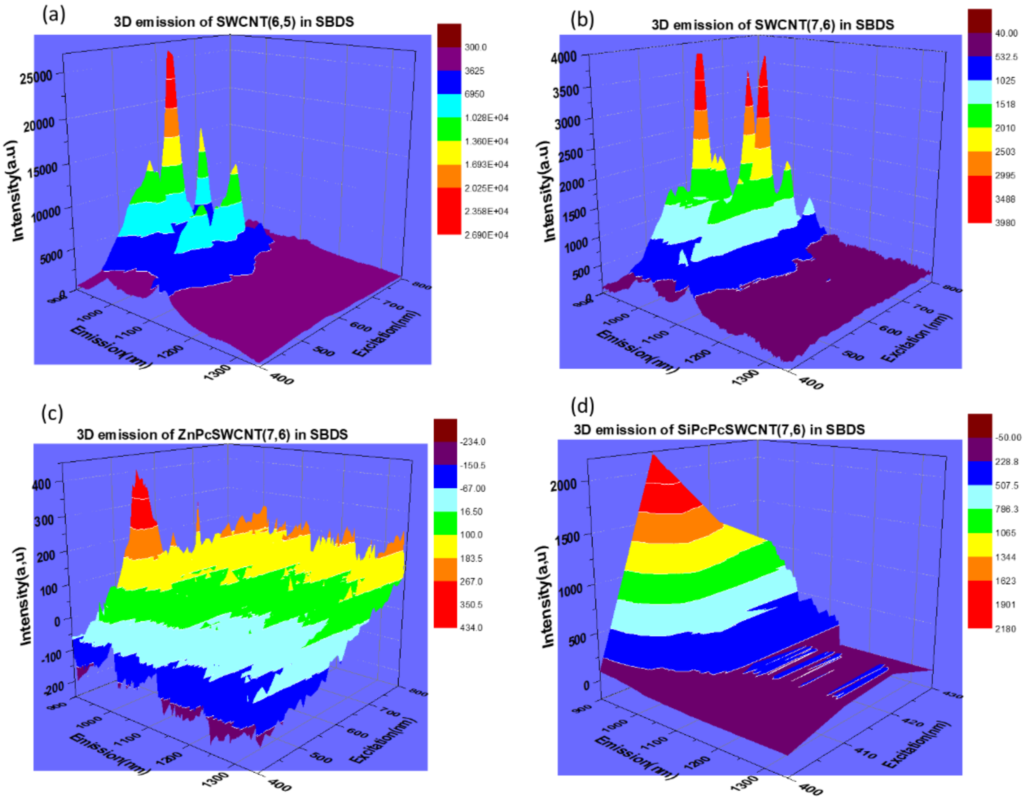

Figure S20. 3- dimensional spectra of (a) SWCNT (6,5), (b) SWCNT (7,6), (c) ZnPc-SWCNT (7,6), and (d) SiPc-SWCNT (7,6) in SBDS.

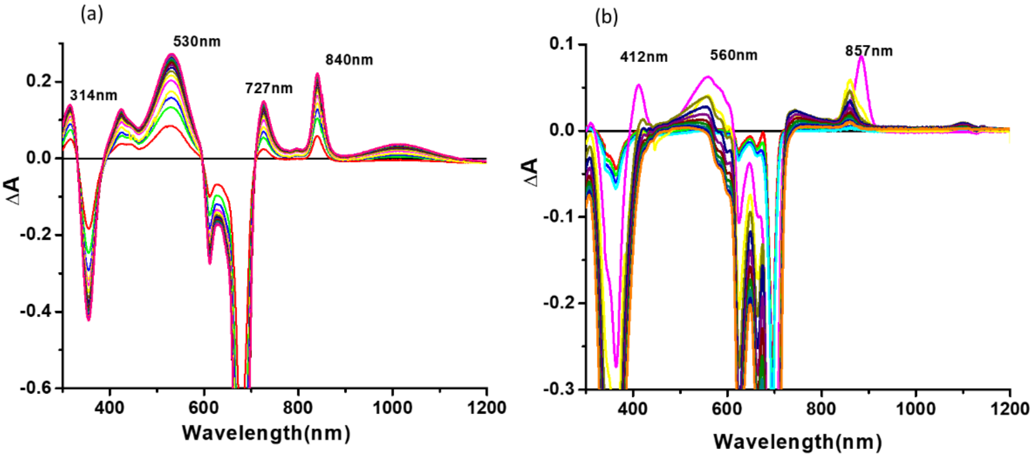

Figure S21. Differential spectra obtained during first oxidation of (a) ZnPc and (b) SiPc control compounds.

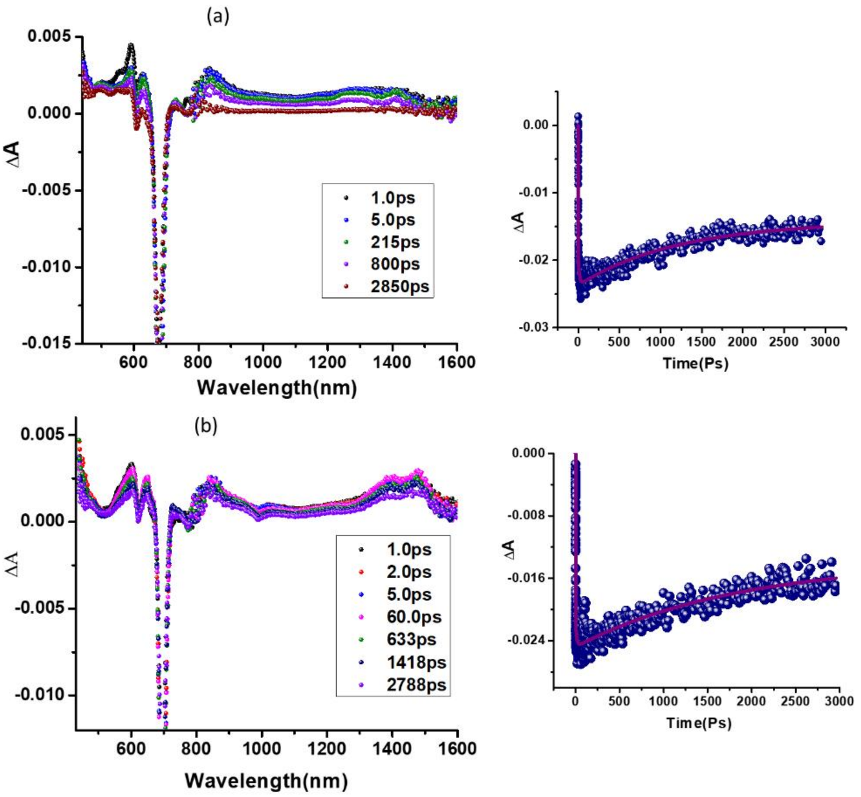

Fig. S22. Femtosecond transient absorption spectra at the indicated delay times of (a) ZnPc and (b) SiPc control compounds in DMF (λ_{ex} = 400 nm). The time profile of the 680 nm peak of ZnPc and 696 nm peak of SiPc are shown at the respective right hand panels.

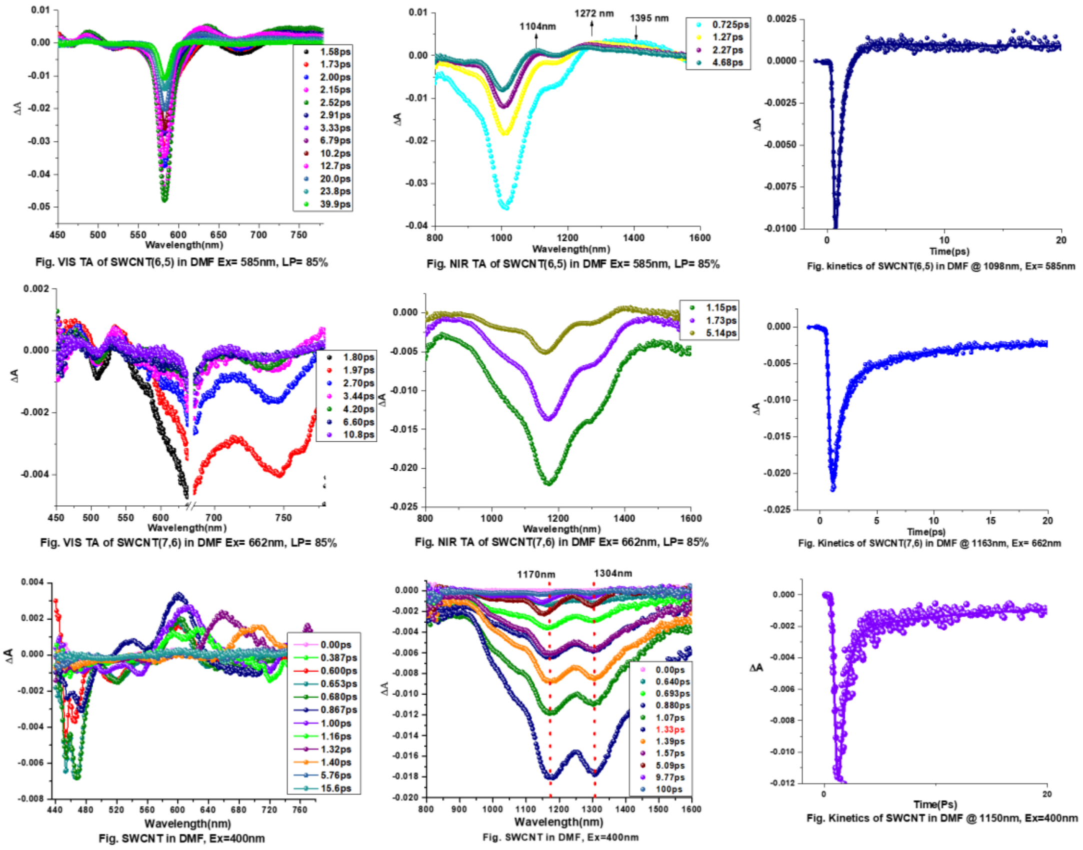

Fig. VIS TA of SWCNT(6,5) in DMF Ex= 585nm, LP= 85%

Fig. NIR TA of SWCNT(6,5) in DMF Ex= 585nm, LP= 85%

Fig. kinetics of SWCNT(6,5) in DMF @ 1098nm, Ex= 585nm

Fig. VIS TA of SWCNT(7,6) in DMF Ex= 662nm, LP= 85%

Fig. NIR TA of SWCNT(7,6) in DMF Ex= 662nm, LP= 85%

Fig. Kinetics of SWCNT(7,6) in DMF @ 1163nm, Ex= 662nm

Fig. SWCNT in DMF, Ex=400nm

Fig. SWCNT in DMF, Ex=400nm

Fig. Kinetics of SWCNT in DMF @ 1150nm, Ex=400nm

Fig. S23. Femtosecond transient absorption spectra of (a) SWCNT (6,5) (b) SWCNT(7,6) and (c) HiPco SWCNT covering the visible (left panels) near-IR region (mid panels) at the indicated delay times in DMF. The right hand panel shows the time profile of excitonic peak of the respective nanotubes.

Table S1. Functionalization data based on TGA results.

Sample	**[a]TGA weight loss (%)**	**[b]Functional group coverage**
ZnPc- SWCNT HiPco	31.4	199
SiPc- SWCNT HiPco	33.4	248
ZnPc- SWCNT (6,5)	39.4	160
SiPc- SWCNT (6,5)	23.7	351
ZnPc-SWCNT (7,6)	31.8	200
SiPc-SWCNT (7,6)	36.2	233

[a] TGA results show relative weight loss. [b] Number of carbon atoms of carbon nanotube skeleton for every functional group added in each reaction.

Table S2: Binding energy (eV) of the core-level atoms of SWCNT samples and its precursors. The peak percentages are indicated in brackets.

	C1s / BE (eV)						**O1s / BE (eV)**		**N1s BE (eV)**		**Si2p BE (eV)**	**$Zn2p_{3/2}$ BE (eV)**	**$I3d_{5/2}$ BE (eV)**
Sample	sp^2 C	sp^3 C	C-O	C=O	COO	π-π*	O=C	O-C	=N-	-NH-			
SWCNT HiPco	284.8 (69)	-	286.2 (22)	287.7 (5)	289.2 (2)	291.3 (2)	531.6 (27)	533.2 (73)	-	-	-	-	-
SWCNT (6,5)	284.8 (69)	-	286.3 (17)	287.8 (11)	-	291.3 (3)	531.3 (6) 532.6 (38)	533.8 (56)	-	-	-	-	-
SWCNT (7,6)	284.8 (67)	-	286.3 (23)	287.8 (7)	-	291.3 (3)	531.3 (21) 532.6 (43)	533.8 (36)	-	-	-	-	-
ZnPc	284.8 (65) 286.3 (10)	285.3 (25)	-	-	-	-	-	-	398.6 (74)	399.9 (26)		1022.3	621.4
SiPc	284.8 (60) 286.3 (3)	285.3 (33)	-	-	289.3 (4)	-	-	-	399.9 (75)	400.2 (25)	103.3	-	621.3
SWCNT-TMS HiPco	284.8 (64)	285.3 (3)	286.3 (26)	287.8 (7)	-	-	532.0 (37)	533.3 (63)	-	-	101.3	-	-
SWCNT (6,5)-TMS	284.8 (68)	285.3 (5)	286.3 (21)	287.8 (6)	-	-	531.3 (14) 532.6 (52)	533.8 (34)	-	-	101.3	-	-
SWCNT (7,6)-TMS	284.8 (69)	-	286.3 (24)	287.8 (7)	-	-	531.3 (13) 532.6 (43)	533.8 (44)	-	-	101.2	-	-
ZnPc-SWCNT HiPco	284.8 (72)	285.3 (3)	286.3 (19)	287.7 (6)	-	-	531.9 (35)	533.4 (65)	399.8 (75)	400.2 (25)	-	1022.1	-

SiPc-SWCNT HiPco	284.8 (70)	285.3 (4)	286.3 (21)	287.7 (5)	-	-	531.8 (39)	533.2 (61)	399.1 (75)	400.2 (25)	103.6	-	-
ZnPc-SWCNT (6,5)	284.8 (66)	285.3 (6)	286.3 (20)	287.8 (8)	-	-	531.3 (20) 532.6 (46)	533.8 (34)	398.1 (75)	400.1 (25)	-	1021.3	-
SiPc-SWCNT (6,5)	284.8 (68)	285.3 (5)	286.2 (21)	287.8 (6)	-	-	531.3 (36) 532.6 (39)	533.8 (25)	398.1 (75)	400.1 (25)	102.6	-	-
ZnPc-SWCNT (7,6)	284.8 (70)	285.3 (5)	286.3 (19)	287.8 (6)	-	-	531.3 (46) 532.6 (34)	533.8 (20)	398.2 (75)	400.1 (25)	-	1021.3	-
SiPc-SWCNT (7,6)	284.8 (64)	285.3 (5)	286.2 (23)	287.8 (8)	-	-	531.3 (28) 532.6 (36)	533.8 (36)	398.1 (75)	400.0 (25)	102.7	-	-

Hyphen means no signal detection

Table S3. Compositional data obtained from the XPS analysis of starting materials (HiPco and enriched SWCNTs), *functionalized* SWCNT and ZnPc and SiPc.

	C (% at)	O (%at)	N (%at)	Si (%at)	Zn (%at)	I (%at)
SWCNT Hipco	95.7	4.3	-	-	-	
SWCNT (6,5)	97.1	2.9	-	-	-	
SWCNT (7,6)	97.5	2.5	-	-	-	
ZnPc	84.6	-	12.5	-	1.4	1.5
SiPc	77.7	6.6	12.2	1.7	-	1.8
SWCNT-TMS HiPco	97.4	2.0	-	0.6	-	-
SWCNT-TMS (6,5)	95.7	2.5	-	1.8	-	-
SWCNT-TMS (7,6)	95.9	2.4	-	1.7	-	-
ZnPc- SWCNT HiPco	93.5	1.9	4.1	-	0.5	-
SiPc- SWCNT HiPco	92.3	3.3	3.9	0.5	-	-
ZnPc-SWCNT (6,5)	94.1	2.4	3.1	-	0.4	-
SiPc- SWCNT(6,5)	83.5	5.8	9.5	1.2	-	-
ZnPc-SWCNT(7,6)	92.5	2.3	4.6	-	0.6	-
SiPc- SWCNT (7,6)	84.7	5.7	8.5	1.1	-	

Table S4. Raman data (G band and 2D band) for *pristine* SWCNTs and *functionalized* samples recorded at 785 nm excitation.

Sample	**G^+ band (cm^{-1})**	**Shift (G^+ band) (cm^{-1})**	**2D band (cm^{-1})**	**Shift (2D band) (cm^{-1})**
SWCNT HiPco	1594	-	2579	-
ZnPc- SWCNT HiPco	1587	7	2574	5
SiPc- SWCNT HiPco	1588	6	2575	4
SWCNT (6,5)	1591	-	2579	-
ZnPc-SWCNT (6,5)	1585	6	2572	7
SiPc- SWCNT (6,5)	1585	6	2569	10
SWCNT (7,6)	1594	-	2578	-
ZnPc-SWCNT (7,6)	1589	5	2567	11
SiPc-SWCNT (7,6)	1591	3	2573	5

References

---

1 A. L. Higginbotham, D.V. Kosynkin, A. Sinitskii, Z. Sun and J. M. Tour, *ACS Nano*, **2010**, *4*, 2059-2069.

2 W. Qi, W. Liu, B. Zhang, X. Gu, X. Guo and D. Su, *Angew. Chem. Int. Ed.,* **2013**, *52*, 14224 -14228.

3 T. S. Olson, S. Pylypenko, J. E. Fulghum and P. Atanassov, *J. Electrochem. Soc*., **2010**, *157*, B54-B63.